Physics Letters B 810 (2020) 135837

Contents lists available at ScienceDirect

Physics Letters B

www.elsevier.com/locate/physletb

Through the looking-glass with ALICE into the quark-gluon plasma: A new test for hadronic interaction models used in air shower simulations

Luis A. Anchordoqui [a,b,c,*], Carlos García Canal [d], Sergio J. Sciutto [d], Jorge F. Soriano [a,b]

[a] Department of Physics and Astronomy, Lehman College, City University of New York, NY 10468, USA
[b] Department of Physics, Graduate Center, City University of New York, NY 10016, USA
[c] Department of Astrophysics, American Museum of Natural History, NY 10024, USA
[d] Instituto de Física La Plata, UNLP, CONICET Departamento de Física, Facultad de Ciencias Exactas, Universidad Nacional de La Plata, C.C. 69, (1900) La Plata, Argentina

ARTICLE INFO

Article history:
Received 13 December 2019
Received in revised form 27 September 2020
Accepted 29 September 2020
Available online 2 October 2020
Editor: A. Ringwald

ABSTRACT

Recently, the ALICE Collaboration reported an enhancement of the yield ratio of strange and multi-strange hadrons to charged pions as a function of multiplicity at mid-rapidity in proton-proton, proton-lead, lead-lead, and xenon-xenon scattering. ALICE observations provide a strong indication that a quark-gluon plasma is partly formed in high multiplicity events of both small and large colliding systems. Motivated by ALICE's results, we propose a new test for hadronic interaction models used for analyzing ultra-high-energy-cosmic-ray (UHECR) collisions with air nuclei. The test is grounded in the almost equal column-energy density in UHECR-air collisions and lead-lead collisions at the LHC. We applied the test to post-LHC event generators describing hadronic phenomena of UHECR scattering and show that these QCD Monte Carlo-based codes must be retuned to accommodate the strangeness enhancement relative to pions observed in LHC data.

Besides addressing key questions in astrophysics, ultra-high-energy cosmic ray (UHECR) experiments provide unique access to particle physics at energies an order-of-magnitude higher center-of-mass energy than pp collisions at the Large Hadron Collider (LHC) [1]. However, a precise characterization of the particle physics properties is usually hampered by the ambiguity of model predictions computed through extrapolation of hadronic interaction models tuned to accommodate collider data. These predictions have sizable differences [2–4], even among modern (post-LHC) models [5], and quite often overlap with the phase of particle physics observables. Disentangling one from the other is of utmost importance to study particle physics in unexplored regions of the phase-space. The development of new approaches to reduce the systematic uncertainties of hadronic interaction models represents one of the most compelling challenges in UHECR data analysis. In this Letter we introduce a reliable technique for extrapolation into the ultra-high-energy domain.

QCD calculations on the Lattice [6] predict that under certain critical conditions of baryon number density and temperature, normal nuclear matter undergoes a phase transition to a deconfined state of quarks and gluons where chiral symmetry is restored [7]. For many purposes, such a quark-gluon plasma (QGP) can be described as a near-perfect fluid with surprisingly large entropy-density-to-viscosity ratio. Therefore, once formed, like any other hot object, the QGP transfers heat internally by radiation. Several phases can be identified during the QGP evolution. The initial state contains only gluons as well as valence u and d quarks, but strangeness is produced in the very early stages via hard (perturbative) $2 \to 2$ partonic scattering processes ($gg \to s\bar{s}$ and $q\bar{q} \to s\bar{s}$). Strangeness is also predominantly produced during the subsequent partonic evolution via gluon splittings ($g \to s\bar{s}$). This is because the very high baryochemical potential inhibits gluons from fragmenting into $u\bar{u}$ and $d\bar{d}$, and therefore they fragment predominantly into $s\bar{s}$ pairs [8]. In the hadronization process that follows this leads to the strong suppression of pions (and hence photons), but allows the production of heavy hadrons with high transverse momentum (p_T) carrying away strangeness. At low p_T non per-

* Corresponding author.
E-mail address: luis.anchordoqui@gmail.com (L.A. Anchordoqui).

https://doi.org/10.1016/j.physletb.2020.135837

turbative processes dominate the production of strange hadrons. Thus, the abundances of strange particles relative to pions provide a powerful discriminator to identify the QGP formation.

A QGP can be created by heating nuclear matter up to a temperature of 2×10^{12} K, which amounts to 175 MeV per particle. Relativistic heavy-ion collisions are then the best tool one has to search for QGP production. Recently, the ALICE Collaboration reported enhancement of the yield ratio of multi-strange hadrons to charged pions as a function of multiplicity at mid-rapidity in LHC proton-proton (pp), proton-lead (pPb), lead-lead (PbPb), and xenon-xenon (XeXe) collisions [9–12]. More concretely:

- the production rate of K^0_S, Λ, ϕ, Ξ, and Ω increases with multiplicity faster than that for charged particles;
- the higher the strangeness content of the hadron, the more pronounced is the increase;
- the ratios do not seem to depend on the system size or collision energies.

Altogether, this provides unambiguous evidence for the formation of a QGP in high multiplicity small and large colliding systems [14].

Now, if the QGP is formed in relativistic heavy-ions collisions one would also expect to be formed in the scattering of UHECRs in the upper atmosphere [15,16]. Moreover, since the column-energy density in UHECR-air collisions is comparable to that in PbPb collisions at the LHC, the precise characterization of the QGP properties from ALICE data enables us to investigate QGP models describing the scattering of cosmic rays that impinge on the Earth's atmosphere with energy $10^9 \lesssim E/\text{GeV} \lesssim 10^{11}$. Indeed, as we show herein ALICE data straightforwardly constrain these models without the need to rely on energy extrapolation.

Before proceeding, we pause to note that the column-energy density is the relevant parameter to compare QGP models with experimental data. This is because in the center-of-mass the particles are extremely Lorentz contracted so the time it takes to pass through each other is small compared to the time for signals to propagate transversely, and hence the pertinent parameter is the total *surface energy density*. The best way of getting this point across is to consider the collision of two nuclei of baryon number A_1 and A_2 in the center-of-mass frame. The energies per nucleon for each nucleus are written as $E_1 = \sqrt{s}/(2A_1)$ and $E_2 = \sqrt{s}/(2A_2)$, where s denotes the total center of mass energy squared. Approximating each nucleus in its rest-frame as a cube of side $L = A^{1/3}$ gives the surface energy density in GeV/nucleon-cross-section [17]

$$\Sigma = A_1^{1/3} E_1 + A_2^{1/3} E_2 = \frac{1}{2}\sqrt{s}\left(A_1^{-2/3} + A_2^{-2/3}\right). \tag{1}$$

Finally, following the de-facto standard of high-energy physics, we rewrite (1) in the nucleon-nucleon center-of-mass frame

$$\Sigma = \frac{1}{4}\sqrt{s_{NN}}\left(A_1^{-2/3} + A_2^{-2/3}\right)(A_1 + A_2), \tag{2}$$

where $\sqrt{s_{NN}} = 2\sqrt{s}/(A_1 + A_2)$ is the center-of-mass energy per nucleon.

For LHC PbPb scattering at $\sqrt{s_{NN}} = 5.02$ TeV we can use (2) to obtain

$$\Sigma^{\text{PbPb}}_{\text{LHC}} = 2.9 \times 10^4 \text{ GeV}, \tag{3}$$

whereas for LHC XeXe scattering at $\sqrt{s_{NN}} = 5.44$ TeV, we have

$$\Sigma^{\text{XeXe}}_{\text{LHC}} = 1.2 \times 10^4 \text{ GeV}. \tag{4}$$

This must be compared to UHECR protons colliding with air nuclei at $10^{10.5} \lesssim s/\text{GeV}^2 \lesssim 10^{12.5}$, which leads to

$$9.8 \times 10^4 < \Sigma^{p\,\text{air}}_{\text{UHECR}}/\text{GeV} < 9.8 \times 10^5, \tag{5}$$

where we have taken $A_{\text{air}} = 14$. For the same primary energy, if the UHECR is a nucleus instead of proton the column energy density is reduced. Now, using (1) it is straightforward to see that for helium and carbon nuclei with $E \gtrsim 10^9$ GeV, $\Sigma^{A\,\text{air}}_{\text{UHECR}} > \Sigma^{\text{PbPb}}_{\text{LHC}}$, but already for nitrogen (and of course nuclei with larger baryon number) there is a particular energy where $\Sigma^{A\,\text{air}}_{\text{UHECR}} \simeq \Sigma^{\text{PbPb}}_{\text{LHC}}$. For example, when a nitrogen with $E \simeq 10^9$ GeV collides with an air nucleus, we have $\sqrt{s_{NN}} \simeq 12$ TeV and a column-energy density $\Sigma^{\text{N air}}_{\text{UHECR}} \simeq 2.9 \times 10^4$ GeV, which is comparable to $\Sigma^{\text{PbPb}}_{\text{LHC}}$. Therefore, under the well justified assumptions of universality between different projectile/target combinations and approximate independence of the collision energy, we conjecture that the QGP model predictions of these two scattering processes must be roughly the same. In particular, both LHC PbPb scattering at $\sqrt{s_{NN}} = 5.02$ TeV and UHECR nitrogen-air collisions at $\sqrt{s_{NN}} \simeq 12$ TeV should produce the same hadron-to-pion yield ratios as a function of the charged multiplicity. The hadron-to-pion yield ratios as a function of the charged multiplicity observed in LHC PbPb scattering at $\sqrt{s_{NN}} = 5.02$ TeV have been reported by the ALICE Collaboration [9–12], providing a direct calibration for hadronic interaction models used for analyzing UHECR collisions with air nuclei.

The column energy density is subject to large fluctuations from collision to collision. For fixed nucleon-nucleon center-of-mass energy, the multiplicity of charged secondary particles is expected to be a reasonable tracer of the column energy density. Large multiplicities correspond to many nucleons interacting (high density), small multiplicities to few nucleons participating in the collision (low density). Taking this argument into account one can perform a comparison of prediction to data as a function of charged particle multiplicity instead of the non-observable column energy density. Because charged multiplicity is a good tracer of the energy density in the collision, the particle ratios are expected to depend on whether the QGP is formed (or not) in the collisions. This is very well seen in the ALICE data [9–12]. High secondary multiplicities correspond to the formation of a larger QGP region than low-multiplicity interactions, as expected. Furthermore, the observed particle ratios are, to a first approximation, only depending on the charged particle multiplicity (in the considered energy range). They are similar for a given charged particle multiplicity and independent of the projectile-target combinations and different nucleon-nucleon center-of-mass energies. This can then be interpreted as reflecting the conjectured dependence on the column energy density.

We now turn to compare the predictions of post-LHC hadronic interaction models (QGSJET II-04 [18], EPOS-LHC [19], and SIBYLL 2.3c [20,21]) with the experimental data reported by the ALICE Collaboration [10]. We run 10^6 collisions for each of the models, pair of primary particles, and center-of-mass energy. In analogy with the analyses presented by the ALICE Collaboration, we select those collisions containing at least one charged particle within the central ($|\eta| < 1$) pseudorapidity region. For those collisions, we first select the charged particles at midrapidity ($|\eta| < 0.5$). To estimate the observable $\langle dN_{\text{ch}}/d\eta\rangle_{|\eta|<0.5}$, we write it as

$$\langle dN_{\text{ch}}/d\eta\rangle_{|\eta|<0.5} = \frac{\int_{|\eta|<0.5} \frac{dN_{\text{ch}}}{d\eta} d\eta}{\int_{|\eta|<0.5} d\eta} = N_{\text{ch}}(|\eta| < 0.5) \equiv N^{\text{c}}_{\text{ch}}, \tag{6}$$

the total number of charged particles at midrapidity which, for the i-th collision, is denoted by $N^{\text{c}}_{\text{ch},i}$. For this collision, we measure the total number of particles $N_{\alpha,i}$ of several groups of species α,

Table 1
Selected particle species α.

α	Particles
π	$\pi^+ + \pi^-$
p	$p^+ + \bar{p}$
K	K^0_S
Λ	$\Lambda + \bar{\Lambda}$
Ξ	$\Xi^- + \bar{\Xi}^+$
Ω	$\Omega^- + \bar{\Omega}^+$

as described in Table 1. Armed with (6), we obtain the ratios to charged pions as

$$\Gamma_{\alpha,i} \equiv \frac{N_{\alpha,i}}{N_{\pi,i}}. \tag{7}$$

In Fig. 1 we show the average ratios $\Gamma_\alpha \equiv \langle \Gamma_{\alpha,i} \rangle$ to all the collisions with the same $N^c_{\rm ch}$ for the six species listed in Table 1 as reported by the ALICE Collaboration. For comparison, we also show the predictions of EPOS-LHC and SIBYLL 2.3c for the above mentioned species (other than ϕ) considering pp collisions $\sqrt{s} = 7$ TeV and $\sqrt{s} = 13$ TeV, as well as NN collisions at $\sqrt{s_{NN}} = 12$ TeV. We note, however, that the particles that play a role on the evolution of UHECR showers are pions, kaons, protons, neutrons, lambdas (and the corresponding antiparticles). For the simulations run with QGSJET, we only display predictions for the relevant secondaries driving the shower evolution. Overall, we conclude that none of the models correctly reproduce the main tendencies of ALICE data, especially for the description of multi-strange hadron production. For pp collisions, all hadronic interaction models seem to reproduce quite well $\Gamma_{p\bar{p}}$ and $\Gamma_{K^0_S}$, but fail to reproduce $\Gamma_{\Lambda\bar{\Lambda}}$. For NN collisions, EPOS-LHC reaches a good enough standard to pass the test in predicting the number of secondary kaons and lambdas as a function of the charge multiplicity. However, $\Gamma_{p\bar{p}}$ is overproduced by roughly 25%. SIBYLL 2.3c provides a good description of $\Gamma_{p\bar{p}}$, but fails to predict the number of kaons and lambdas. Finally, QGSJET slightly overproduces $\Gamma_{p\bar{p}}$ and fails to predict $\Gamma_{K^0_S}$ and $\Gamma_{\Lambda\bar{\Lambda}}$. All in all, EPOS-LHC provides the best description of the hadron-to-pion yield ratios as a function of the charged multiplicity relevant in the modeling of UHECR shower evolution. Of course, if QGP effects are correctly implemented in the models they should describe the aforementioned features as seen in data.

We end with three observations:

- Over the last year there has been a tremendous amount of progress in modeling UHECR interactions with EPOS-LHC [22]. In particular, the new EPOS-QGP has been properly tuned to reproduce the particle to pion ratio for the Ω baryon versus multiplicity at mid-rapidity as reported by the ALICE Collaboration [23,24]. It will be interesting to see whether the EPOS-QGP predictions of NN collisions at $\sqrt{s_{NN}} = 12$ TeV can accurately match the experimental data of $\Gamma_{p\bar{p}}$.
- Future LHC data (including pO and OO collisions [25]) will provide new insights to guide software development.
- The formation of a QGP could play a significant role in the development of UHECR air-showers. In particular, the enhanced production of multi-strange hadrons in high-multiplicity small and large colliding systems would suppress the fraction of energy which is transferred to the electromagnetic shower-component. The formation of QGP blobs in air showers would then enhance the number of muons reaching ground level, and would also modify the shape of the muon density distribution $\rho_\mu(r)$. The curvature of this distribution ($d^2\rho_\mu/dr^2$) has been proposed as a possible discriminator between hadronic interaction models with sufficient statistics [26]. A thorough study of these phenomena is underway and will be presented elsewhere.

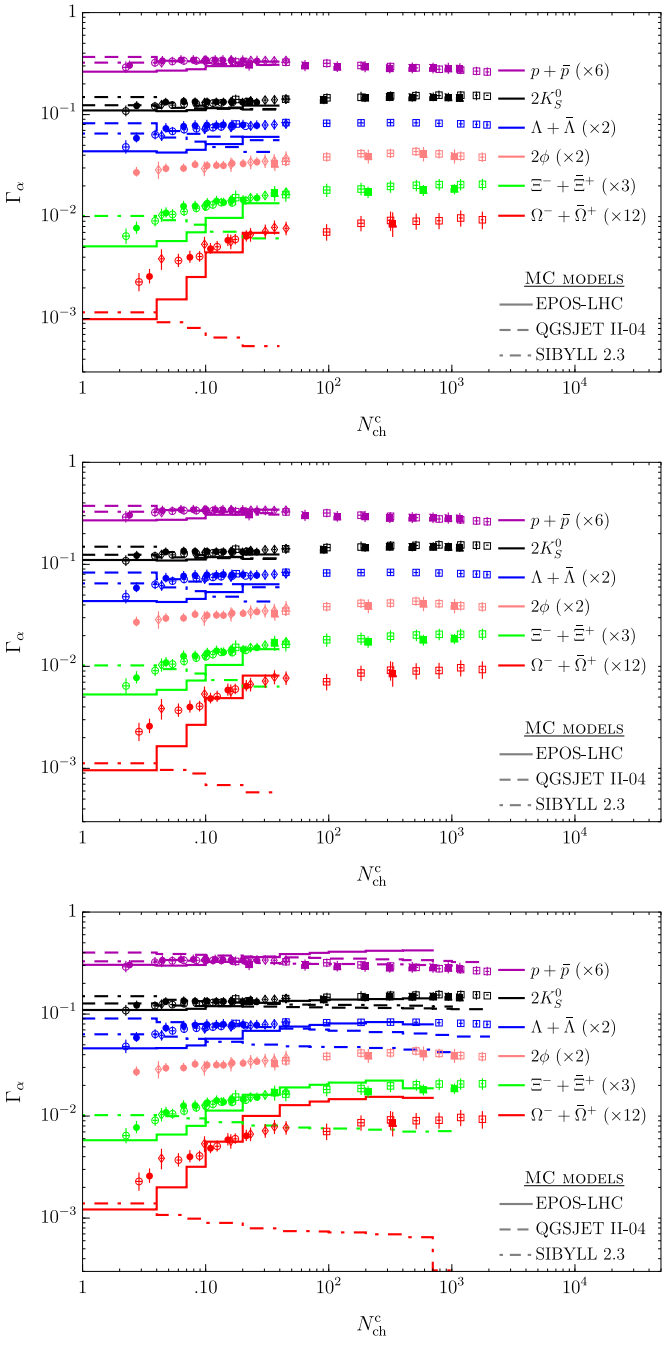

Fig. 1. Hadron-to-pion yield ratios as a function of the charged particle multiplicity in pp, pPb, PbPb, and XeXe collisions at the LHC. The predictions of post-LHC hadronic interaction models (top-to-bottom, pp $\sqrt{s} = 7$ TeV, pp $\sqrt{s} = 13$ TeV, NN $\sqrt{s_{NN}} = 12$ TeV) are compared to data reported by the ALICE Collaboration: ∘ pp at $\sqrt{s} = 7$ TeV, • pp $\sqrt{s} = 13$ TeV, ◇ pPb at $\sqrt{s_{NN}} = 5.02$ TeV, □ PbPb at $\sqrt{s_{NN}} = 5.02$ TeV, ■ XeXe at $\sqrt{s_{NN}} = 5.44$ TeV [10]. (We have corrected a factor of two which is missing in the labeling of $\Gamma_{\Lambda\bar{\Lambda}}$ in Fig. 6 of [10], Fig. 4 of [11], Fig. 1 of [12], and Fig. 1 of [13].)

Declaration of competing interest

Declaration of Interests: none.

Acknowledgements

We thank Prabi Palni and Francesco Noferini for valuable email communication. L.A.A. and J.F.S. are supported by U.S. National Science Foundation (NSF Grant PHY-1620661) and by the National

Aeronautics and Space Administration (NASA 80NSSC18K0464). C.G.C. and S.J.S. are partially supported by ANPCyT.

References

[1] L.A. Anchordoqui, Ultra-high-energy cosmic rays, Phys. Rep. 801 (2019) 1, https://doi.org/10.1016/j.physrep.2019.01.002, arXiv:1807.09645 [astro-ph.HE].

[2] L.A. Anchordoqui, M.T. Dova, L.N. Epele, S.J. Sciutto, Hadronic interactions models beyond collider energies, Phys. Rev. D 59 (1999) 094003, https://doi.org/10.1103/PhysRevD.59.094003, arXiv:hep-ph/9810384.

[3] R. Ulrich, R. Engel, M. Unger, Hadronic multiparticle production at ultra-high energies and extensive air showers, Phys. Rev. D 83 (2011) 054026, https://doi.org/10.1103/PhysRevD.83.054026, arXiv:1010.4310 [hep-ph].

[4] D. d'Enterria, R. Engel, T. Pierog, S. Ostapchenko, K. Werner, Constraints from the first LHC data on hadronic event generators for ultra-high energy cosmic-ray physics, Astropart. Phys. 35 (2011) 98, https://doi.org/10.1016/j.astropartphys.2011.05.002, arXiv:1101.5596 [astro-ph.HE].

[5] L. Calcagni, C.A. García Canal, S.J. Sciutto, T. Tarutina, LHC updated hadronic interaction packages analyzed up to cosmic-ray energies, Phys. Rev. D 98 (8) (2018) 083003, https://doi.org/10.1103/PhysRevD.98.083003, arXiv:1711.04723 [hep-ph].

[6] S. Borsanyi, G. Endrodi, Z. Fodor, A. Jakovac, S.D. Katz, S. Krieg, C. Ratti, K.K. Szabo, The QCD equation of state with dynamical quarks, J. High Energy Phys. 1011 (2010) 077, https://doi.org/10.1007/JHEP11(2010)077, arXiv:1007.2580 [hep-lat].

[7] E.V. Shuryak, Quantum chromodynamics and the theory of superdense matter, Phys. Rep. 61 (1980) 71, https://doi.org/10.1016/0370-1573(80)90105-2.

[8] J. Rafelski, B. Muller, Strangeness production in the quark-gluon plasma, Phys. Rev. Lett. 48 (1982) 1066, https://doi.org/10.1103/PhysRevLett.48.1066, Erratum: Phys. Rev. Lett. 56 (1986) 2334, https://doi.org/10.1103/PhysRevLett.56.2334.

[9] J. Adam, et al., ALICE Collaboration, Enhanced production of multi-strange hadrons in high-multiplicity proton-proton collisions, Nat. Phys. 13 (2017) 535, https://doi.org/10.1038/nphys4111, arXiv:1606.07424 [nucl-ex].

[10] P. Palni, ALICE Collaboration, Multiplicity dependence of strangeness and charged particle production in proton-proton collisions, arXiv:1904.00005 [nucl-ex].

[11] F. Noferini, ALICE highlights, MDPI Proc. 13 (2019) 6, https://doi.org/10.3390/proceedings2019013006, arXiv:1906.02460 [hep-ex].

[12] R. Vertesi, ALICE Collaboration, Overview of recent ALICE results, Contribution to: EDS Blois 2019 arXiv:1910.01981 [nucl-ex].

[13] M. Sharma, ALICE Collaboration, Strangeness production in p–Pb collisions at 8.16 TeV, arXiv:1911.04845 [hep-ex].

[14] P. Koch, B. Müller, J. Rafelski, From strangeness enhancement to quark–gluon plasma discovery, Int. J. Mod. Phys. A 32 (31) (2017) 1730024, https://doi.org/10.1142/S0217751X17300241, arXiv:1708.08115 [nucl-th].

[15] G.R. Farrar, J.D. Allen, A new physical phenomenon in ultra-high energy collisions, EPJ Web Conf. 53 (2013) 07007, https://doi.org/10.1051/epjconf/20135307007, arXiv:1307.2322 [hep-ph].

[16] L.A. Anchordoqui, H. Goldberg, T.J. Weiler, Strange fireball as an explanation of the muon excess in Auger data, Phys. Rev. D 95 (6) (2017) 063005, https://doi.org/10.1103/PhysRevD.95.063005, arXiv:1612.07328 [hep-ph].

[17] G.R. Farrar, Particle physics at ultrahigh energies, arXiv:1902.11271 [hep-ph].

[18] S. Ostapchenko, Monte Carlo treatment of hadronic interactions in enhanced pomeron scheme I: QGSJET-II model, Phys. Rev. D 83 (2011) 014018, https://doi.org/10.1103/PhysRevD.83.014018, arXiv:1010.1869 [hep-ph].

[19] T. Pierog, I. Karpenko, J.M. Katzy, E. Yatsenko, K. Werner, EPOS LHC: test of collective hadronization with data measured at the CERN Large Hadron Collider, Phys. Rev. C 92 (3) (2015) 034906, https://doi.org/10.1103/PhysRevC.92.034906, arXiv:1306.0121 [hep-ph].

[20] A. Fedynitch, F. Riehn, R. Engel, T.K. Gaisser, T. Stanev, The hadronic interaction model Sibyll-2.3c and inclusive lepton fluxes, arXiv:1806.04140 [hep-ph].

[21] R. Engel, A. Fedynitch, T.K. Gaisser, F. Riehn, T. Stanev, The hadronic interaction model Sibyll 2.3c and extensive air showers, arXiv:1912.03300 [hep-ph].

[22] T. Pierog, B. Guiot, I. Karpenko, G. Sophys, M. Stefaniak, K. Werner, EPOS 3 and air showers, EPJ Web Conf. 210 (2019) 02008, https://doi.org/10.1051/epjconf/201921002008.

[23] S. Baur, H. Dembinski, T. Pierog, R. Ulrich, K. Werner, The ratio of electromagnetic to hadronic energy in high energy hadron collisions as a probe for collective effects, and implications for the muon production in cosmic ray air showers, arXiv:1902.09265 [hep-ph].

[24] T. Pierog, S. Baur, H. Dembinski, R. Ulrich, K. Werner, Collective hadronization and air showers: can LHC data solve the muon puzzle?, PoS ICRC 2019 (2019) 387.

[25] Z. Citron, et al., Report from Working Group 5: future physics opportunities for high-density QCD at the LHC with heavy-ion and proton beams, https://doi.org/10.23731/CYRM-2019-007.1159, arXiv:1812.06772 [hep-ph].

[26] L. Anchordoqui, H. Goldberg, Footprints of super-GZK cosmic rays in the Pilliga State Forest, Phys. Lett. B 583 (2004) 213, https://doi.org/10.1016/j.physletb.2003.12.072, arXiv:hep-ph/0310054.